

A transmandibular lateral transsphenoidal navigated surgical approach to access a pituitary macroadenoma in a warmblood mare

Mathieu de Preux, Christina Precht, Julien Guevar, Claudia Graubner, Sebastian Thenhaus-Schnabel, Larissa Buser, Anton Lukes & Christoph Koch

To cite this article: Mathieu de Preux, Christina Precht, Julien Guevar, Claudia Graubner, Sebastian Thenhaus-Schnabel, Larissa Buser, Anton Lukes & Christoph Koch (2024) A transmandibular lateral transsphenoidal navigated surgical approach to access a pituitary macroadenoma in a warmblood mare, *Veterinary Quarterly*, 44:1, 1-10, DOI: [10.1080/01652176.2023.2300947](https://doi.org/10.1080/01652176.2023.2300947)

To link to this article: <https://doi.org/10.1080/01652176.2023.2300947>



© 2024 Swiss Institute of Equine Medicine (ISME), Department of Clinical Veterinary Medicine, Vetsuisse-Faculty, University of Bern, Bern, Switzerland. Published by Informa UK Limited, trading as Taylor & Francis Group



Published online: 23 Feb 2024.



Submit your article to this journal [↗](#)



Article views: 43



View related articles [↗](#)



View Crossmark data [↗](#)

A transmandibular lateral transsphenoidal navigated surgical approach to access a pituitary macroadenoma in a warmblood mare

Mathieu de Preux^a, Christina Precht^b, Julien Guevar^c, Claudia Graubner^a, Sebastian Thenhaus-Schnabel^b, Larissa Buser^d, Anton Lukes^e and Christoph Koch^a

^aSwiss Institute of Equine Medicine (ISME), Department of Clinical Veterinary Medicine, Vetsuisse-Faculty, University of Bern, Bern, Switzerland; ^bDivision of Clinical Radiology, Department of Clinical Veterinary Medicine, Vetsuisse-Faculty, University of Bern, Bern, Switzerland; ^cDepartment of Surgery, Small Animal Clinic, Vetsuisse-Faculty, University of Bern, Bern, Switzerland; ^dDivision of Anaesthesiology and Pain Management, Department of Clinical Veterinary Medicine, Vetsuisse-Faculty, University of Bern, Bern, Switzerland; ^eDepartment of Neurosurgery, Lindenhof Hospital, Bern, Switzerland

ABSTRACT

A 16-year-old warmblood mare was referred with a progressive history of behavioral changes and left-sided blindness. Following neuroanatomical localization to the forebrain, magnetic resonance imaging of the head revealed a well-delineated, 4.5 cm in diameter, round pituitary mass causing marked compression of the midbrain and optic chiasm. Euthanasia was recommended but declined by the owners. Veterinary specialists and a human neurosurgeon collaboratively prepared for surgical case management. A novel navigated transmandibular lateral transsphenoidal approach was developed to access the region of the sella turcica and practiced on cadaver specimens. The horse was anesthetized and placed in sternal recumbency with the head above the heart line. Using a cone beam computed tomography (CBCT)-coupled navigation system, a navigated pin traversing the vertical ramus of the mandible and the lateral pterygoid muscle was placed in a direct trajectory to the predetermined osteotomy site of the basisphenoid bone. A safe corridor to the osteotomy site was established using sequential tubular dilators bypassing the guttural pouch, internal and external carotid arteries. Despite the use of microsurgical techniques, visualization of critical structures was limited by the long and narrow working channel. Whilst partial resection of the mass was achieved, iatrogenic trauma to the normal brain parenchyma was identified by intraoperative imaging. With consent of the owner the mare was euthanized under the same general anesthesia. Post-mortem magnetic resonance imaging and gross anatomical examination confirmed partial removal of a pituitary adenoma, but also iatrogenic damage to the surrounding brain parenchyma, including the thalamus.

ARTICLE HISTORY

Received 23 August 2023
Accepted 26 December 2023

KEYWORDS



Horse; pituitary adenoma; computer-assisted surgery; neuronavigation; pituitary pars intermedia dysfunction

1. Introduction

Pituitary pars intermedia dysfunction (PPID) is the most frequently encountered endocrine disease in the geriatric horse (Brosnahan and Paradis 2003; Miller et al. 2016), with an estimated prevalence of 21.2% in horses and ponies 15 years and older (McGowan et al. 2013). Clinical signs of PPID in equids include hypertrichosis, laminitis, epaxial muscle wastage, weight loss, polydipsia, polyuria, and lethargy or depression (Ireland and McGowan 2018). In most affected equids, the pars intermedia of the pituitary gland becomes grossly enlarged, consistent with macroadenoma formation (Heinrichs et al. 1990). This may eventually lead to compression of the pars distalis of the adenohypophysis, the neurohypophysis (Heinrichs et al. 1990), the hypothalamus, and the optic chiasm, resulting in various additional clinical

signs, ranging from hormonal imbalances to neurological deficits and blindness (Van der Kolk et al. 1993; Wallace et al. 1996; Daoualibi et al. 2020). Therapy is most often medical with oral pergolide mesylate. Although clinical improvement is seen in about 75% of affected horses (Tatum et al. 2020), lifelong daily dosage is required and mass effects of large tumors are not reduced or eliminated (Pease et al. 2011).

Although surgical approaches to the equine brain are described in the literature (Allen et al. 1987; Comelisse et al. 2001; Janicek et al. 2006; Kramer et al. 2007; Broux et al. 2019), intracranial surgery is rarely performed in horses. Apart from a ventral transsphenoidal osteotomy to approach the equine pituitary gland (Carmalt and Scansen 2018) there is no available literature as how to access the ventral

CONTACT Mathieu de Preux  mathieu.depreux@unibe.ch  Swiss Institute of Equine Medicine, Länggassstrasse 124, Postfach 8466, CH-3001 Bern, Switzerland

© 2024 Swiss Institute of Equine Medicine. Published by Informa UK Limited, trading as Taylor & Francis Group

This is an Open Access article distributed under the terms of the Creative Commons Attribution-NonCommercial License (<http://creativecommons.org/licenses/by-nc/4.0/>), which permits unrestricted non-commercial use, distribution, and reproduction in any medium, provided the original work is properly cited. The terms on which this article has been published allow the posting of the Accepted Manuscript in a repository by the author(s) or with their consent.

or ventrolateral aspect of the skull and specifically the pituitary gland in horses. In humans, the treatment of choice for ACTH-dependent hyperadrenocorticism (true Cushing disease) caused by an adenoma is curative by transnasal transsphenoidal hypophysectomy (Biller et al. 2008). Similar surgical principles are also used in dogs and cats *via* a transoral approach (Meij et al. 2002). In both humans (Eboli et al. 2011; Achey et al. 2019; Patil et al. 2021) and small animals (Owen et al. 2018; Winger 2014), the use of computer assisted surgery has been shown to reduce the risks of iatrogenic collateral damage while improving the extent of tumor resection and remission rate during curative transnasal transsphenoidal hypophysectomy.

In this case report, we describe a novel navigated, transmandibular lateral transsphenoidal approach to a pituitary macroadenoma in a warmblood mare and the attempted surgical removal of the tumor.

2. Case history

A 16-year-old, 562 kg Selle-Français mare was presented to the ISME Equine Clinic Bern, Vetsuisse Faculty of the University of Bern, Switzerland for a chronic progressive history of abnormal mentation, behavior and left-sided blindness.

3. Clinical findings and further investigation

The clinical evaluation was unremarkable other than hypertrichiosis accentuated over the extremities. The neurological examination identified an abnormal mental status with severe obtundation and poor response to external stimuli and head pressing. Posture was abnormal with an extension of the neck and a low head carriage and circling towards the left side. Menace response was absent on the left, negative ipsilateral (left eye) and contralateral pupillary light reflexes, and a bilateral horizontal nystagmus with a rapid phase towards the left on the left eye and towards the right on the right eye. Mild proprioceptive deficits and ataxia were observed as

circumduction and hypermetria of the pelvic limbs. The ataxia dramatically worsened when the mare was forced to walk with her head kept in an elevated position (grade 3 Mayhew ataxia scale). Neuroanatomical localization was to the brain, involving the visual pathway.

A complete hematology and serum biochemistry was performed and revealed no significant abnormalities. Baseline plasma ACTH concentrations were elevated (82.2 ng/L, reference value December-June < 40 ng/L). The response to the subsequent TRH stimulation test was also abnormally elevated (268.0 ng/L 10 min after stimulation, reference value < 110 ng/L), confirming the diagnosis of PPID. Based on these findings, a pituitary macroadenoma was suspected and confirmed by MRI of the head (3 Tesla MRI unit, Magnetom Vida, Siemens Healthcare AG, Zürich, Switzerland) with the finding of a large (4.5 × 4.6 × 4.2 cm), well-delineated, spherical space-occupying, diffusely heterogeneously moderately contrast-enhancing, and associated with a strongly enhancing peripheral rim mass lesion at the level of the pituitary fossa causing marked compression of the thalamus, midbrain, and optic chiasm, compatible with a pituitary macroadenoma (Figure 1).

Given the severity of the neurological signs associated with the tumor, which was deemed inoperable because of its size and location, euthanasia was recommended. The owner, however, firmly declined euthanasia and the mare was uneventfully recovered from general anesthesia after MRI examination.

4. Surgical case management

4.1. Development of the surgical approach and special equipment

In an interdisciplinary collaboration of human and small animal neurosurgeons, radiologists, anesthesiologists, and equine surgeons, a novel surgical approach was proposed, tailored to the specific size and anatomy of an equine patient. Considerations included the shortest working distance possible to allow for the use of a surgical microscope or rigid scope, but

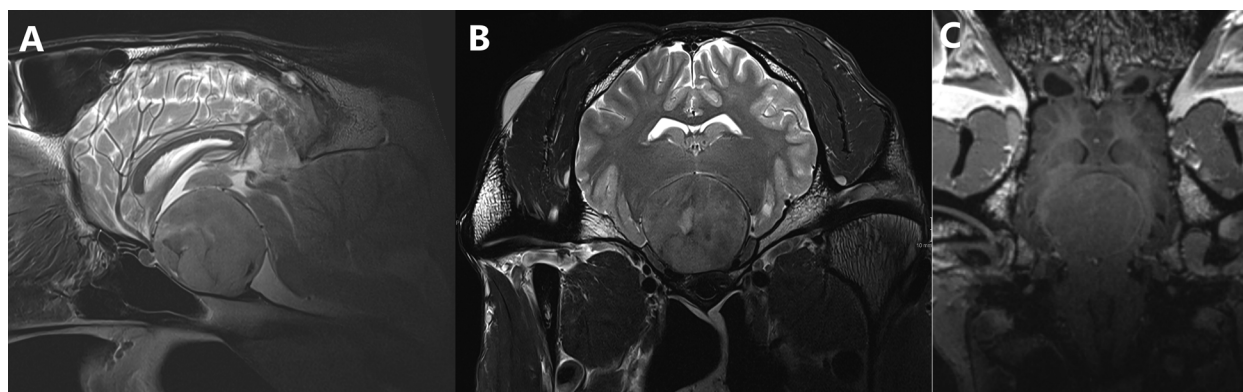


Figure 1. (A) T2w sagittal, (B) T2w transverse and (C) T1w 3D reconstructable magnetization-prepared gradient-echo (MP-RAGE) with contrast medium (gadoteric acid, clariscan™, GE Healthcare AG, opfikon, Switzerland) dorsal magnetic resonance images of the head of a 16-year-old warmblood mare, depicting a large well-delineated pituitary macroadenoma compressing the thalamus, the midbrain, and the optic chiasm.

also the safest access possible to avoid the abundant neurovascular structures at the ventral aspect of the cranium and near the foramen lacerum, as well as the contaminated respiratory mucosa of the guttural pouch. A transmandibular, lateral transsphenoidal approach was therefore elected by performing a fenestration of the vertical ramus of the mandible and then traverse the lateral pterygoid muscle and access the lateral aspect of the basisphenoid bone.

The available surgical equipment included a high-speed drill (Midas Rex M8, Medtronic), sequential muscle dilators (METRx II System, Medtronic) and magnification (surgical microscope (Leica Microsystems GmbH, Wetzlar, Germany) and/or rigid endoscope (Karl Storz Endoscopy, Tuttlingen, Germany)). The O-arm 2 and the StealthStation S8 (Medtronic, Louisville, Colorado) were used for neuro-navigation. Prior training and evaluation of the technique and instruments were performed on cadaveric equine head specimens obtained from two horses euthanatized for reason unrelated to the topic of this case report and donated by their owner by signing an informed consent. The experimental nature of the surgery was agreed upon by the owner.

4.2. Patient preparation

Prior to induction of general anesthesia, the horse was fasted for 12h while given access to water. Prophylactic antimicrobials, including benzylpenicillin sodium (30'000 IU/kg, Penicillin Natrium Streuli, Streuli Pharma AG) and gentamicin sulfate (6.6 mg/kg, Pargenta-50, Dr E Graeb AG), were administered intravenously (IV) along with flunixin meglumine (1.1 mg/kg, Vetaflumex, Provect AG). Sedation was achieved using romifidine (0.06 mg/kg IV, Sedivet, Boehringer Ingelheim) and levomethadone (0.05 mg/kg IV, L Polamivet, MSD Animal Health GmbH). The mare was carefully placed in a full-body Animal Rescue and Transportation Sling (ARTS, size L) (Fürst et al. 2008) and secured to a hoist.

General anesthesia was induced by administering ketamine (2.5 mg/kg IV, Ketazol-100, Dr E Graeb AG) and diazepam (0.05 mg/kg IV, Valium, Roche Pharma AG), and the horse was gently positioned in a sternal position on the padded floor within the induction box to allow for transoral endotracheal intubation (OD 28 mm.). Subsequently, the anesthetized horse was hoisted and positioned in sternal recumbency over a surgical mattress placed on the surgery table (Haico pro 3 equine operating table, Avante animal health, Louisville, USA). The front and hind limbs were left lying on both sides of the mattress, adopting freely a slightly flexed posture (Figure 2). The mare's head was placed on a carbon fiber table (Opera Swing; General Medica Merate SPA, Seriate, Italy) and positioned in a vacuum cushion slightly tilted to the right to improve surgical site exposure while keeping it elevated above heart level to reduce intracranial pressure and intraoperative bleeding (Brosnan et al. 2002). General anesthesia was

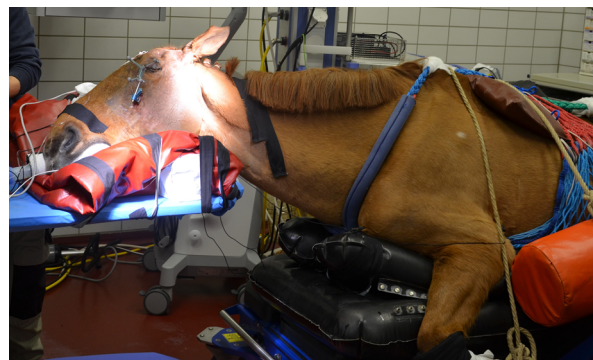


Figure 2. Photograph showing the mare positioned in sternal recumbency on the surgery table, with her head placed in an elevated position on a carbon fiber table. The patient tracker required for surgical navigation using an optical tracking system is solidly anchored on the left facial crest using two 3.2 mm Schanz pins.

maintained with sevoflurane vaporized in O₂ and medical air (FiO₂ 0.9–1), supplemented with constant rate infusions of ketamine (1 mg/kg/h IV, Ketazol-100, Dr E Graeb AG) and romifidine (0.03 mg/kg/h IV, Sedivet, Boehringer Ingelheim). Intermittent positive pressure ventilation was applied throughout anesthesia using a large animal anesthesia machine (Tafonius, Vetronic, UK). Ventilation settings were adjusted to maintain the end-tidal CO₂ between 35 and 40 mmHg. Ringer Lactate solution (Ringer Lactate, Bichsel, Interlaken, Switzerland) and dobutamine were administered as needed (0–1 µg/kg/min IV, Dobutrex TEVA Pharma AG, Basel, Switzerland), ensuring mean and systolic arterial pressures (right transverse facial artery) remained above 70 and 110, respectively. Standard physiological variables were monitored (Tafonius, Vetronic, UK) continuously, and arterial blood gas and chemical analyses were performed approximately every hour. In addition, the electroencephalogram was monitored in the operating room (SedLine®, Masimo Corp., CA, USA) and the density spectral array monitoring was continuously recorded. During aseptic preparation, a single episode of severe bradycardia (18–20 beats per minute) occurred without an identifiable cause. This resolved with the administration of atropine (0.01 mg/kg IV, Sintetica 1 mg/mL, Mendrisio, Switzerland).

Following aseptic preparation of the left cheek, the bridge of the nose and the periocular region, the patient tracker (passive orthopedic reference frame 963–864 and fixator 9730864, StealthStation System, Medtronic, Louisville, Colorado) was anchored on the left facial crest using two 3.2 mm self-tapping Schanz pins inserted through stab incisions (Figure 2). Furthermore, the cornea was moistened with eye ointment containing retinyl palmitate (Vitamin A <Blache>, Bausch & Lomb Swiss AG, Switzerland) and a temporary tarsorrhaphy was performed on the left eye with two simple interrupted sutures with absorbable monofilament suture material (Monocryl 2–0, Ethicon, Johnson & Johnson) to avoid cornea drying during the surgical procedure. The upper and lower incisors were wired shut using two loops of

1.25 mm stainless-steel wire to avoid alteration of the spatial relationship between the patient tracker, the cranium, and the mandible. In the same position, the horse was subsequently moved into the surgical theatre.

4.3. Preoperative imaging

After an additional aseptic preparation and draping of the surgical field, the mobile CBCT unit and the coupled navigation system (O-arm 2 and StealthStation S8, both Medtronic) were moved into position so that the camera of the optical tracking system simultaneously detected the reflecting spheres of the patient tracker and the infrared light-emitting tracker of the gantry. The gantry position was adjusted until the region occupied by the spherical mass was centered in the field of view. Correct gantry positioning was repeatedly checked using the integrated 2D fluoroscopic function. A high-definition CBCT scan was acquired using 120 kV, an exposure of 125 mA, and an acquisition time of 27 s. The resulting 192 transverse isotropic images were automatically exported to the navigation system. The CBCT dataset (as well as all subsequent intraoperative CBCT scans) was merged with the T1-weighted 3D MP-RAGE sequence acquired ten days before surgery, which had been manually imported from the PACS (Deep unity, Dedalus, Bonn, Germany) to the navigation system. The acquired CBCT images were reviewed by a radiologist to ensure that the area of interest, i.e. the entire length of the anticipated approach and the adenoma, were included. The gantry was opened, and the mobile CBCT unit was pulled out of the operating theatre to give the operating surgeons full access to the surgical site.

4.4. Surgical planning

Patient registration was performed by placing the tip of a sharp navigated pointer (Passive Planar Probe (sharp), 960–553, StealthStation System, Medtronic) in the divot of the patient tracker. The navigated pointer and its virtual projection were then used to define the surgical approach on the merged CBCT and MRI dataset on the StealthStation S8. The trajectory for the planned surgical approach traversed the left masseter muscle and the thin part of the vertical ramus of the mandible in an oblique rostroventral to caudodorsal direction, midway between its rostral and caudal edges, dorsal to the large maxillary vein on the medial aspect of the mandible, and about 5 cm ventral to the temporomandibular joint. Medial to the mandible, the trajectory of the planned surgical approach was to lay within the lateral pterygoid muscle, taking care to avoid penetration of the ventrally located guttural pouch. The target area of the planned surgical approach was the surface of the basisphenoid bone about 2 cm rostral to the foramen lacerum, just caudal to the caudal alar foramen and

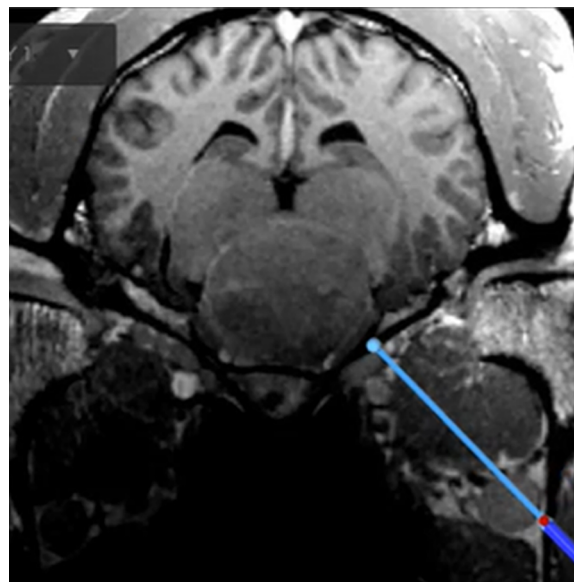


Figure 3. Close-up view of a screen shot of the StealthStation S8 depicting the surgical plan on merged cone beam computed tomography and T1w high-resolution 3D reconstructable magnetization-prepared gradient-echo (3D MP-RAGE) transverse plane images. The light blue line represents the core axis of the corridor to be established as transmandibular lateral transsphenoidal surgical approach to the pituitary macroadenoma.

3 cm dorsal to the muscular tubercle. A final criterium for the surgical plan was that the trajectory of the surgical plan was close to the center of the pituitary macroadenoma (Figure 3)

4.5. Surgical procedure

A 10 cm curved, rostrally convex skin incision was made over the caudal edge of the left vertical mandibular ramus, extending ventrally from a point just ventral to the temporomandibular joint. The buccal branches of the facial nerve were cautiously elevated through tunneling of the superficial fascia of the masseter muscle with Metzenbaum scissors from ventral to dorsal, and isolated with a Penrose drain. The aponeurosis of the masseter muscle close to the caudal rim of the vertical ramus of the mandible was sharply transected and the masseter muscle was bluntly separated from the underlying mandible with a periosteal elevator and retracted rostral and dorsal. A navigated high-speed drill (Midas Rex MR8, Medtronic) was used to create a circular fenestration of approximately 3 cm diameter centered on the thin portion of the mandible where the trajectory of the predefined surgical plan penetrated the mandible (Figure 4). Fenestration was started at the dorsal edge of the planned bone corridor and progressively enlarged towards ventral, taking care not to damage the maxillary vein.

The 0.0625 × 12" guidewire of the METRx II System (Medtronic) was introduced under navigation guidance penetrating the now exposed lateral pterygoid muscle until it firmly contacted the basisphenoid

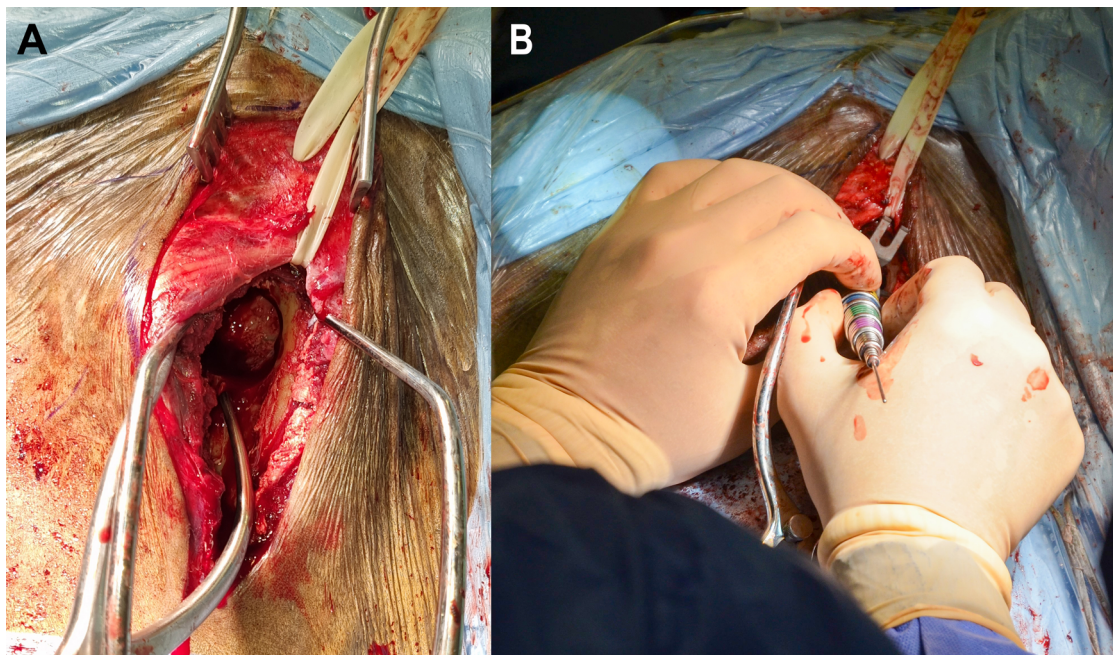


Figure 4. (A) Intraoperative photograph of the surgical approach performed in the left cheek to gain access to the lateral pterygoid muscle through a circular osteotomy in the vertical ramus of the mandible (rostral is to the left, dorsal is to the top of the image). The buccal branches of the facial nerve are protected by a Penrose drain. (B) Insertion of the sequential muscle dilators (METRx II System, Medtronic) in the lateral pterygoid muscle through the osteotomy to create a working channel to gain access to the basisphenoid bone. Please note the central guidewire, the tip of which is firmly contacting the basisphenoid bone.

bone. At this point, a first intraoperative CBCT scan was run to confirm correct placement of the guidewire. Based on these images, the position of the guidewire had to be slightly corrected rostrally and dorsally until alignment with the trajectory of the predefined surgical plan was obtained. A working channel was created in the center of the lateral pterygoid muscle by sequentially inserting the dilators of the METRx II System over the guidewire while maintaining firm contact between the tip of the guidewire and the basisphenoid bone (Figure 4). The largest dilator that could be inserted had an inner diameter of 18.8mm and a length of 9cm. This dilator ultimately served as a speculum to create the osteotomy in the basisphenoid bone and thus establish the surgical approach to the cranium.

Several attempts were made to visualize the surface of the basisphenoid bone with the operating microscope through the dilator. Although the microscope provided an excellent magnification to examine the deep structures, it had to be positioned too close to the dilator to focus, thus preventing the introduction of surgical instruments. Therefore, the microscope was replaced by a 30° forward oblique, 4mm outer diameter, 18cm standard telescope (Karl Storz Endoscopy, Tuttlingen, Germany) for illumination and magnification of the surgical field.

The remaining fibers of the lateral pterygoid muscle covering the lateral surface of the basisphenoid bone were transected using a 15cm long electrode connected to a radiofrequency unit (VAPR Tripolar 90° Suction Electrode, DePuy Synthes, Johnson & Johnson, 22851 Norderstedt, Deutschland). Finally, a

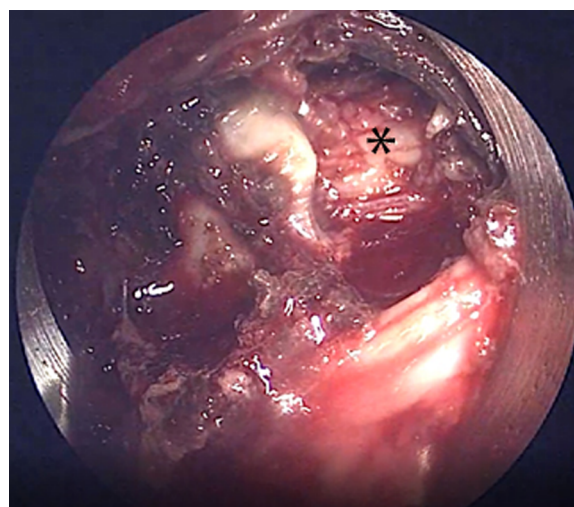


Figure 5. Intraoperative view of the circular osteotomy in the basisphenoid bone, provided by a 30° forward oblique, 4mm outer diameter, 18cm standard telescope (Karl Storz Endoscopy, Tuttlingen, Germany) inserted in the metallic muscle dilator. The maxillary branch of the trigeminal nerve (*) is visible in the sulcus nervi maxillaris through the osteotomy.

circular, 15mm in diameter osteotomy of the basisphenoid bone was created under navigation guidance using the high-speed drill. The dorsal edge of the maxillary branch of the trigeminal nerve (V2) was visible in the sulcus nervi maxillaris through the osteotomy (Figure 5). Based on the MRI dataset, the pituitary adenoma would have been located just axial and dorsal to this structure. However, the

tumor could not be visualized and identified as such with the endoscope. Moreover, the long and narrow dilator made adequate intracranial instrumentation impossible when using the available equipment. This limitation prevented intracranial accurate tissue dissection and surgical resection of the tumor under direct visual control.

A Ferris-Smith rongeur mounted with an instrument tracker (SureTrak II Universal Tracker, Large Passive Fighter, 961–581, Medtronic) was then introduced into the center of the tumor under navigation guidance. A second intraoperative CBCT scan confirmed the correct placement of the rongeur, and a tissue sample was harvested for histopathological examination, which later confirmed the suspected diagnosis of a pituitary macroadenoma. Despite the lack of visual control, careful attempts were made to resect as much tumor tissue as possible with various surgical instruments, all mounted with an instrument tracker. For intraoperative orientation during those attempts, the surgeons were left to rely exclusively on the merged CBCT and MRI images displayed on the screen of the navigation system. Following these attempts, a third intraoperative CBCT scan revealed large intracranial gas accumulations indicating successful partial removal of the adenoma, but also iatrogenic trauma to the brain parenchyma, including portions of the adjacent tissue of the thalamus. Hence, it was decided to not let the horse recover from surgery, because detrimental effects on vital cognitive capabilities were expected. With the consent of the owner, the mare was euthanized on the table.

Importantly, intraoperatively neither uncontrollable hemorrhage nor anesthesia-related complications occurred. The total anesthesia duration was 365 min, with the $\text{PaO}_2/\text{FiO}_2$ ratio remaining above 485 mmHg. No abnormal electrical activity was reported on the EEG. The horse had a mean patient state index of 20 (unitless) and a mean suppression ratio also of 20% over the surgical procedure. Following euthanasia,

the integrity of the guttural pouch was confirmed using a flexible endoscope.

A post-mortem MRI of the head confirmed partial resection of the left laterorostral quadrant of the pituitary mass lesion, with the created void being partially filled with gas and coagulated blood, respectively. In addition, the adjacent left thalamus also showed a defect filled with gas, which confirmed inadvertent iatrogenic damage to the brain parenchyma (Figure 6). The surgical approach presented as a collapsed track with gas accumulations in the left masseteric and lateral pterygoid muscle and bone defects in the left mandible and left basisphenoid bone. In the corridor left of the surgical approach, the first (N. ophthalmicus, V1) and second (N. maxillaris, V2) branches of the fifth cranial nerve (N. trigeminus) were focally lost. Also, the maxillary branch of the external carotid artery could not be delineated focally. The internal carotid artery was well defined, located caudally to the surgical approach.

Finally, the head was cut in a transverse plane to anatomically illustrate the path of the surgical approach (Figure 7).

5. Discussion

The management of pituitary pars intermedia dysfunctions is essential in equine practice and gaining importance due to the high prevalence of this pathology in geriatric horses and the growing proportion of aged equids in the population (Ireland et al. 2011; Welsh et al. 2016). Most of these cases are successfully managed with daily oral administration of pergolide mesylate. However, there is currently no therapy for cases unresponsive to medical treatment, such as horses suffering from neurological deficits induced by space-occupying macroadenoma compressing the adjacent tissues. This case report describes the surgical access to a large macroadenoma in a warmblood mare and its attempted

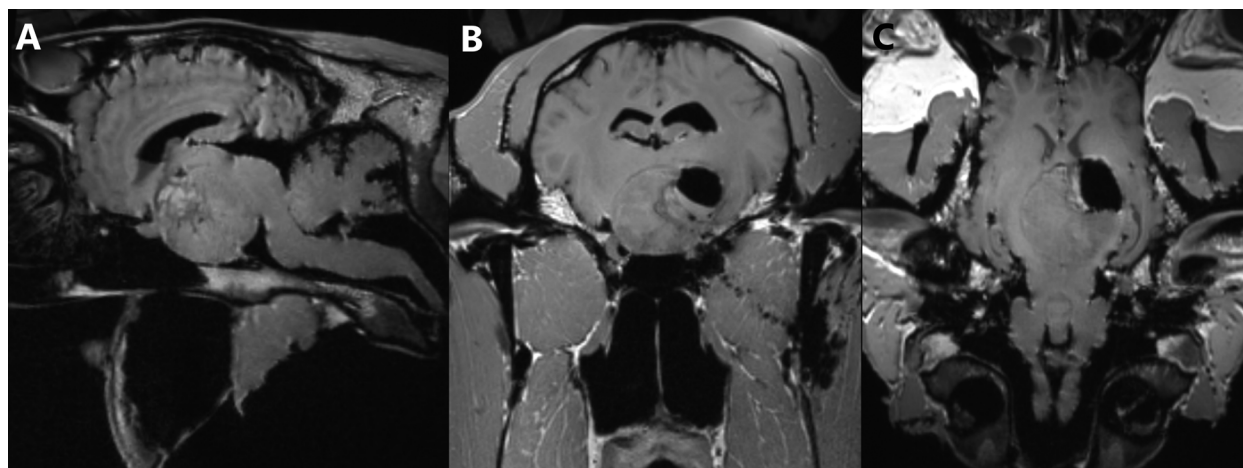


Figure 6. Post-mortem T1w high-resolution 3D reconstructable magnetization-prepared gradient-echo (3D MP-RAGE), (A) transverse, (B) sagittal and (C) dorsal plane magnetic resonance images of the head of a 16-year-old warmblood mare, depicting partial removal of the adenoma, but also inadvertent removal of portions of the thalamus.



Figure 7. Post-mortem transverse slice of the head of the warmblood mare depicting the left-sided transmandibular lateral transsphenoidal surgical approach providing access to the pituitary macroadenoma. Parts of the mass had been removed intraoperatively, as demonstrated by the hemorrhagic area in its left dorsal aspect (right in the image), but iatrogenic damages to the surrounding brain parenchyma are also macroscopically visible. Please note the hemorrhagic tract within the center of the lateral pterygoid muscle, where the sequential muscle dilators were inserted.

removal. The anesthetized horse was positioned in sternal recumbency, with the head above the heart line and slightly tilted to the right, to lower the intracranial pressure and enable the surgeons to work in a convenient position. Neither excessive intraoperative bleeding nor anesthesia-related complications were recorded during the procedure. Whilst surgery was not successfully completed, the novel navigated transmandibular lateral transsphenoidal approach allowed for a controlled access to the tumor.

The transnasal transsphenoidal approach, which is used to access the region of the pituitary gland in humans and dogs, was soon discarded because of the dimensions and the dolichocephalic shape of the equine head. In human neurosurgery, microsurgical anatomy references provided by Rhoton's work (Rhoton 2019) are helpful for planning and understanding the benefits and risks of any surgical approach to that area. Such microsurgical anatomy references are lacking in equine surgery. Previously reported experiences with a series of equine cadaveric specimen trials to access the pituitary gland (Carmalt and Scansen 2018) encouraged us to look for alternative approaches. In the latter, the ventral aspect of the basisphenoid bone was accessed through a standard laryngotomy (Ducharme et al.

2019), followed by penetration of the guttural pouches. Based on the CBCT and MRI datasets, the estimated length of this approach would have been 20 cm (from the cricothyroid membrane to the basisphenoid bone), compared to a length of 6,5 cm for the lateral approach (from the mandible to the basisphenoid bone). The ventral approach was therefore deemed inadequate for several reasons: (1) its depth, (2) the exposure to the contaminated respiratory mucosa of the guttural pouch, (3) the risk of iatrogenic damage to the internal carotid artery running in the roof of the medial compartment of the guttural pouch, and (4) the lack of protective tissue layers covering the osteotomy after the intervention. The tissue dilators allowed to establish a working channel traversing the lateral pterygoid muscle while safely retracting the major blood vessels including the external carotid artery and its continuation, the maxillary artery, which is running in close vicinity through the caudal alar foramen into the alar canal. The lateral pterygoid muscle not only provides a direct, broad, and safe corridor to the basisphenoid bone, but also an expected good post-operative soft tissue seal of the osteotomy site, potentially lowering the risk for surgical site infection. Further potential advantages of the lateral approach compared to the ventral osteotomy is the higher versatility for the removal of large, dorsally expansile tumors, as the lateral fenestration of the basisphenoid bone can be extended dorsally and not only provides access to the floor of the sella turcica.

One potential limitation of the here described lateral approach might be the restricted access to the ventral and contralateral aspects of the space occupied by a large mass. To reach these regions, special long, curved or angled instruments may become necessary. Alternatively, a more invasive lateral approach combined with a mandibular condylectomy would provide a more direct trajectory and potentially better access to these regions. Although we considered a mandibular condylectomy and taking a more invasive approach, this idea was soon abandoned. This decision was based on weighing potential benefits against the presumed added risks for iatrogenic damage and the morbidity associated with the condylectomy.

In the case presented here, the adenoma seemed well-delineated on magnetic resonance images. However, a complete surgical excision of the tumor would have been an unrealistic goal due to its large diameter and its firm consistency, i.e. not liquefied as this is often the case in humans. Furthermore, the obliquity of the left-sided surgical approach precluded access to its right most ventral aspect, and the narrowness and length of the approach precluded blind dissection guided by tactile feedback. Therefore, the stated primary goal was to remove at least the dorsal portion of the adenoma to transiently improve the clinical signs by decompressing the surrounding structures.

The main reason for the abortion of the surgical procedure was the inability to appropriately

illuminate and magnify the deep surgical field, which resulted in poor visualization of the adenoma, and thus prevented the identification of a safe tissue plane for dissection. Visual control throughout the entire procedure would have been essential to avoid inadvertent iatrogenic damage to the surrounding brain parenchyma, the vasculature, and the branches of the trigeminal nerve. Soft tissue dissection relying exclusively on the merged CBCT and MRI datasets is doomed to fail because of distortion of the initial spatial relationship following penetration of the cranium, cerebrospinal fluid outflow after opening the cisterns and manipulation of the intracranial structures. Resection of the tumor tissues will inevitably lead to a collapse of surrounding brain parenchyma into the created void and lead to significant mismatch of the visual soft-tissue information provided by the navigation, which is based on the pre-operatively acquired MRI-scans. Moreover, the resulting brain shift invalidates the patient-to-image mapping (Gerard et al. 2017).

The surgical operating microscope would have provided adequate visualization of the intracranial structures, but it was almost in direct contact with the inserted dilator when reaching adequate focus, which impaired the introduction of the available instruments. Specific instrumentation, for example long, bayoneted instruments would have been required to work through this channel. The use of a microscope with a longer working distance (i.e. over 400 mm) or the insertion of a shorter dilator would have solved this technical issue. Furthermore, the insertion of a shorter, and thus wider, sequential dilator of the METRx II System would have allowed further dorsal extension of the circular basisphenoid osteotomy, which could have improved accessibility of the adenoma. Several attempts were made to insert a shorter and wider dilator. These attempts were not successful, although the fenestration in the mandible appeared large enough to accommodate it. In retrospect we speculate that the insertion of a wider dilator was not possible in the clinical case because the maximum stretching capacity of the lateral pterygoid muscle had been reached. This speculation is supported by the fact that it was possible to introduce a shorter and wider dilator in the cadaver specimens used for developing and practicing the approach.

As soon as it became clear that the long inserted dilator impeded the use of the available operating microscope, the microscope was replaced by a telescope. The illumination and magnification provided by the telescope were still not adequate to reliably identify the boundaries of the adenoma. Furthermore, the short working distance of the telescope also precluded proper surgical instrumentation. In the future, this technical limitation could be overcome with the use of a telescope with a longer shaft and a longer working distance (i.e. 250 mm), as reported for transphenoidal removal of pituitary adenomas in dogs (Mamelak et al. 2014). In summary, technical refinements (like the use of shorter dilators, surgical

operating microscopy with a longer working distance, specific telescope, and bayoneted instruments), may allow for controlled manipulation of intracranial tissue in horses and should therefore be further explored. In addition, the use of selective tissue ablation technologies, such as ultrasonic cavitation devices, would enhance intracranial tissue ablation safety in cases where the intraoperative visualization remains limited.

Advanced imaging techniques like CT and MRI are increasingly available in equine referral centers. This not only improves the diagnostic capacities to identify intracranial pathologies but also paves the way for image-guided therapeutic options. Computer-assisted surgery has now become well-established in human neurosurgery and for various indications, for example skull-base surgery (Tzelnick et al. 2023). Technological advances will continue to further improve the already impressive surgical accuracy achieved by modern surgical navigation systems and provide increasingly user-friendly solutions for veterinary surgeons to fully appreciate the benefits of real-time intraoperative anatomical and instrumental orientation. Equine surgeons are only starting to explore the possibilities of surgical navigation (Heer et al. 2019; de Preux et al. 2020; de Preux et al. 2022; Greim et al. 2023). In our case, the main incentive for using surgical navigation was to accurately gain access to a predefined location in the basisphenoid bone while minimizing the inherent risks of traumatizing vital structures, such as the maxillary vein, the guttural pouch and the internal and external carotid arteries. The detailed information on bony and soft tissue structure provided by the merged CBCT and MRI datasets and real-time intraoperative orientation provided by the surgical navigation, proved particularly useful to safely place the central pin of the dilator system.

In conclusion, this case report describes a novel navigated approach to the equine basisphenoid bone to access a pituitary macroadenoma causing severe neurological signs. To date, this is the only description of a navigated surgical approach to the ventrolateral aspect of the equine cranium, which provides access to previously unreachable intracranial structures. The technical limitations encountered during the attempted removal of the tumor may be overcome in the future with the help of additional specialized equipment for illumination and magnification of the surgical field, as well as selective tissue ablation. Further work is needed to refine the technique and assess the repeatability of the approach. Ultimately, in the absence of reported clinical experience of partial adenomectomy in horses, the consequences of such a surgical procedure on the physiological homeostasis of the equine patient and the risk of recurrence of the clinical signs remain to be determined.

Acknowledgments

The authors thank Suzanne Petit and Christoph Tschantré for technical support during the surgical procedure.

Furthermore, the authors thank Sabine Kässmeyer and Kati Hänssgen for their help in the post-mortem preparation of the head.

Disclosure statement

No potential conflict of interest was reported by the author(s).

Funding

The author(s) reported there is no funding associated with the work featured in this article.

References

- Achey RL, Karsy M, Azab MA, Scoville J, Kundu B, Bowers CA, Couldwell WT. 2019. Improved surgical safety via intraoperative navigation for transnasal transsphenoidal resection of pituitary adenomas. *J Neurol Surg B Skull Base*. 80(6):626–631. doi:10.1055/s-0039-1677677.
- Allen JR, Barbee D, Boulton C, Major M, Crisman M, Murnane R. 1987. Brain abscess in a horse: diagnosis by computed tomography and successful surgical treatment. *Equine Vet J*. 19(6):552–555. doi:10.1111/j.2042-3306.1987.tb02672.x.
- Billir BMK, Grossman AB, Stewart PM, Melmed S, Bertagna X, Bertherat J, Buchfelder M, Colao A, Hermus AR, Hofland LJ, et al. 2008. Treatment of adrenocorticotropic-dependent Cushing's syndrome: a consensus statement. *J Clin Endocrinol Metab*. 93(7):2454–2462. doi:10.1210/jc.2007-2734.
- Brosnahan MM, Paradis MR. 2003. Demographic and clinical characteristics of geriatric horses: 467 cases (1989–1999). *J Am Vet Med Assoc*. 223(1):93–98. doi:10.2460/javma.2003.223.93.
- Brosnan RJ, Steffey EP, LeCouteur RA, Imai A, Farver TB, Kortz GD. 2002. Effects of body position on intracranial and cerebral perfusion pressures in isoflurane-anesthetized horses. *J Appl Physiol*. 92(6):2542–2546. doi:10.1152/japplphysiol.00055.2002.
- Broux B, van Bergen T, Schauvliege S, Vali Y, Lefère L, Gielen I. 2019. Successful surgical debridement of a cerebral *Streptococcus equi equi* abscess by parietal bone flap craniotomy in a 2-month-old Warmblood foal. *Equine Vet Educ*. 31(10):e58–e62. doi:10.1111/eve.12995.
- Carmalt JL, Scansen BA. 2018. Development of two surgical approaches to the pituitary gland in the Horse. *Vet Q*. 38(1):21–27. doi:10.1080/01652176.2017.1415488.
- Comelisse CJ, Li HCS, Lowrie CT, Rosenstein DS. 2001. Successful treatment of intracranial abscesses in 2 horses. *Veterinary Internal Medicine*. 15(5):494–500. doi:10.1111/j.1939-1676.2001.tb01581.x.
- Daoualibi Y, Rocha JF, de Farias Brito M, da Silva Alonso L, Ubiali DG. 2020. Central blindness associated with a pituitary adenoma in a mare. *Acta Scientiae Vet*. 48 doi:10.22456/1679-9216.100106.
- de Preux M, Klopfenstein Bregger MD, Brünisholz HP, Van der Vekens E, Schweizer-Gorgas D, Koch C. 2020. Clinical use of computer-assisted orthopedic surgery in horses. *Vet Surg*. 49(6):1075–1087. doi:10.1111/vsu.13486.
- de Preux M, van der Vekens E, Racine J, Sangiorgio D, Klopfenstein Bregger MD, Brünisholz HP, Koch C. 2022. Accessory carpal bone fracture repair by means of computer-assisted orthopaedic surgery in a Warmblood stallion. *Equine Vet Educ*. 34(11):e478–e484. doi:10.1111/eve.13594.
- Ducharme NG, Cheetham J, Pharynx. 2019. Pharynx. In: Auer JA, Stick JA, Kümmerle JM, Prange T, editors. *Equine surgery*, 5th ed. St. Louis (MO): Elsevier. p. 710–733.
- Eboli P, Shafa B, Mayberg M. 2011. Intraoperative computed tomography registration and electromagnetic neuro-navigation for transsphenoidal pituitary surgery: accuracy and time effectiveness. *J Neurosurg*. 114(2):329–335. doi:10.3171/2010.5.JNS091821.
- Fürst AE, Keller R, Kummer M, Manera C, Von Salis B, Auer J, Bettschart-Wolfensberger R. 2008. Evaluation of a new full-body animal rescue and transportation sling in horses: 181 horses (1998–2006). *J Vet Emerg Crit Care*. 18(6):619–625. doi:10.1111/j.1476-4431.2008.00366.x.
- Gerard LJ, Kersten-Oertel M, Petrecca K, Sirhan D, Hall JA, Collins DL. 2017. Brain shift in neuronavigation of brain tumors: a review. *Med Image Anal*. 35:403–420. doi:10.1016/j.media.2016.08.007.
- Greim E, de Preux M, Koch C, Petruccione I, Klopfenstein Bregger MD, van der Vekens E, Brünisholz H. 2023. Computer-assisted removal of an ectopic tooth from the mandibular fossa through a mandibular condylectomy approach in a Comptois gelding. *Equine Vet Educ*. 35(5):e364–e371. doi:10.1111/eve.13742.
- Heer C, Fürst A, Del Chicca F, Jackson MA. 2019. Comparison of 3D-assisted surgery and conservative methods for treatment of type III fractures of the distal phalanx in horses. *Equine Vet Educ*. 32(S10):42–51. doi:10.1111/eve.13232.
- Heinrichs M, Baumgärtner W, Capen C. 1990. Immunocytochemical demonstration of proopiomelanocortin-derived peptides in pituitary adenomas of the pars intermedia in horses. *Vet Pathol*. 27(6):419–425. doi:10.1177/030098589902700606.
- Ireland J, Clegg P, McGowan C, McKane S, Pinchbeck G. 2011. A cross-sectional study of geriatric horses in the United Kingdom. Part 1: demographics and management practices. *Equine Vet J*. 43(1):30–36. doi:10.1111/j.2042-3306.2010.00145.x.
- Ireland JL, McGowan CM. 2018. Epidemiology of pituitary pars intermedia dysfunction: a systematic literature review of clinical presentation, disease prevalence and risk factors. *Vet J*. 235:22–33. doi:10.1016/j.tvjl.2018.03.002.
- Janicek JC, Kramer J, Coates JR, Lattimer JC, LaCarrubba AM, Messer NT. 2006. Intracranial abscess caused by *Rhodococcus equi* infection in a foal. *J Am Vet Med Assoc*. 228(2):251–253. doi:10.2460/javma.228.2.251.
- Kramer J, Coates JR, Hoffman AG, Frappier BL. 2007. Preliminary anatomic investigation of three approaches to the equine cranium and brain for limited craniectomy procedures. *Vet Surg*. 36(5):500–508. doi:10.1111/j.1532-950X.2007.00297.x.
- Mamelak AN, Owen TJ, Bruyette D. 2014. Transsphenoidal surgery using a high definition video telescope for pituitary adenomas in dogs with pituitary dependent hypercortisolism: methods and results. *Vet Surg*. 43(4):369–379. doi:10.1111/j.1532-950X.2014.12146.x.
- McGowan T, Pinchbeck G, McGowan C. 2013. Prevalence, risk factors and clinical signs predictive for equine pituitary pars intermedia dysfunction in aged horses. *Equine Vet J*. 45(1):74–79. doi:10.1111/j.2042-3306.2012.00578.x.
- Meij B, Voorhout G, Rijnberk A. 2002. Progress in transsphenoidal hypophysectomy for treatment of pituitary-dependent hyperadrenocorticism in dogs and cats.

- Mol Cell Endocrinol. 197(1-2):89–96. doi:[10.1016/s0303-7207\(02\)00283-6](https://doi.org/10.1016/s0303-7207(02)00283-6).
- Miller M, Moore G, Bertin F, Kritchevsky J. 2016. What's new in old horses? Postmortem diagnoses in mature and aged equids. *Vet Pathol.* 53(2):390–398. doi:[10.1177/0300985815608674](https://doi.org/10.1177/0300985815608674).
- Owen TJ, Chen AV, Frey S, Martin LG, Kalebaugh T. 2018. Transsphenoidal surgery: accuracy of an image-guided neuronavigation system to approach the pituitary fossa (sella turcica). *Vet Surg.* 47(5):664–671. doi:[10.1111/vsu.12906](https://doi.org/10.1111/vsu.12906).
- Patil NR, Dhandapani S, Sahoo SK, Chhabra R, Singh A, Dutta P, Walia R, Verma R, Gupta R, Virk RS, et al. 2021. Differential independent impact of the intraoperative use of navigation and angled endoscopes on the surgical outcome of endonasal endoscopy for pituitary tumors: a prospective study. *Neurosurg Rev.* 44(4):2291–2298. doi:[10.1007/s10143-020-01416-x](https://doi.org/10.1007/s10143-020-01416-x).
- Pease A, Schott H, Howey E, Patterson J. 2011. Computed tomographic findings in the pituitary gland and brain of horses with pituitary pars intermedia dysfunction. *J Vet Intern Med.* 25(5):1144–1151. doi:[10.1111/j.1939-1676.2011.00784.x](https://doi.org/10.1111/j.1939-1676.2011.00784.x).
- Rhoton AL Jr 2019. *Rhoton's cranial anatomy and surgical approaches*. Oxford: Oxford University Press.
- Tatum R, McGowan C, Ireland J. 2020. Efficacy of pergolide for the management of equine pituitary pars intermedia dysfunction: a systematic review. *Vet J.* 266:105562. doi:[10.1016/j.tvjl.2020.105562](https://doi.org/10.1016/j.tvjl.2020.105562).
- Tzelnick S, Rampinelli V, Sahoavaler A, Franz L, Chan HHL, Daly MJ, Irish JC. 2023. Skull-Base Surgery—A Narrative Review on Current Approaches and Future Developments in Surgical Navigation. *J Clin Med.* 12(7):2706. doi:[10.3390/jcm12072706](https://doi.org/10.3390/jcm12072706).
- Van der Kolk J, Kalsbeek H, Van Garderen E, Wensing T, Breukink H. 1993. Equine pituitary neoplasia: a clinical report of 21 cases (1990-1992). *Vet Rec.* 133(24):594–597.
- Wallace M, Crisman M, Pickett J, Carrig C, Sponenburg D. 1996. Central blindness associated with a pituitary adenoma in a horse. *Equine Practice.* 18:8–13.
- Welsh CE, Duz M, Parkin TD, Marshall JF. 2016. Prevalence, survival analysis and multimorbidity of chronic diseases in the general veterinarian-attended horse population of the UK. *Prev Vet Med.* 131:137–145. doi:[10.1016/j.pre-vetmed.2016.07.011](https://doi.org/10.1016/j.pre-vetmed.2016.07.011).
- Wininger F. 2014. Neuronavigation in small animals: development, techniques, and applications. *Veter Clin Small Anim Pract.* 44(6):1235–1248.